Fermi National Accelerator Laboratory

FERMILAB-Conf-92/129-E

Recent Experimental Studies of Hadron Showers Produced in High Energy Muon-Nucleus Interactions

J. Morfin

Fermi National Accelerator Laboratory
P.O. Box 500, Batavia, Illinois 60510

May 1992

Contributed to the XXI International Symposium on Multiparticle Dynamics, Wuhan, China, September 23-27, 1991.

Disclaimer

RECENT EXPERIMENTAL STUDIES OF HADRON SHOWERS PRODUCED IN HIGH ENERGY MUON-NUCLEUS INTERACTIONS

Jorge G. Morfín
Fermi National Laboratory
Batavia, IL 60510
U.S.A.

The Fermilab Tevatron Muon Experiment has analyzed the hadron showers of events resulting from the scattering of a muon beam ($< E_\mu >$ = 490 GeV) off H_2, D_2 and Xenon targets. The topics which will be discussed are: 1. space-time evolution of the hadronization process; 2. leading hadron distributions in the shadowing region; 3. rates and characteristics of 3-jet events.

1. Introduction

Recent results in the study of lepto-produced hadronic showers have been dominated by experiments using incoming muons with energy ranging from 100 GeV to 500 GeV. These include the following:

I) Fermilab Tevatron Muon Experiment (E-665)
II) CERN European Muon Collaboration
III) CERN New Muon Collaboration

Since the Tevatron Muon Collaboration results are both the most recent and in a new, higher-energy regime, this paper will concentrate on those results and refer to the other experiments only for comparison.

Contribution to the XXI International Symposium on Multiparticle Dynamics, Wuhan, China, September 23-27, 1991

1.1 Notation

The standard picture of inelastic muon scattering is shown below

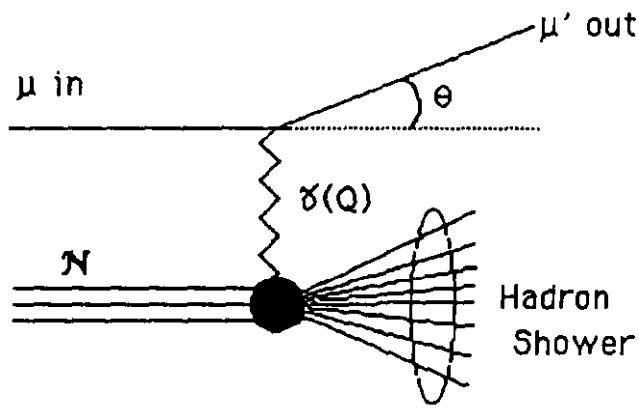

Fig 1. Feynman Graph representation of inelastic muon scattering

In discussing the phenomena of deeply inelastic scattering, there are standard kinematic variables used to characterize the interaction. If the incoming muon has energy E while the scattered muon has energy E' and scattering angle θ then the amount of 4-momentum transferred to the struck quark is:

$$Q^2 = 4EE'\sin^2 \theta/2 = -q^2$$

The transferred energy is

$$\upsilon = E - E'$$

with relative energy transfer

$$y = \upsilon / E$$

The ratio of the 4-momentum transferred to the energy transferred is a measure of the fraction of the total nucleon momentum carried by the struck quark, as first formulated by Bjorken;

$$x_{Bj} = Q^2 / 2M\upsilon .$$

The hadronic shower is described by the effective mass of the shower

$$W^2 = M^2 + 2M\upsilon - Q^2,$$

and individual hadrons within the shower are characterized by the ratio of the hadron's energy to the total energy transferred to the hadron system

$$z = p / p_{max} = E_h / \upsilon .$$

The transverse momentum (p_t) of the hadron is with respect to the direction

of the virtual photon.

Feynman-x relates a hadron's 3-momentum to the 3-momentum of the photon propagator, and the rapidity of a hadron is a measure of it's direction relative to the photon propagator's direction;

$$x_F = \frac{P_L^*}{(P_L^*)_{max}}$$

$$Y = 0.5 \ln \frac{E + P_L}{E - P_L}$$

2. The Fermilab Tevatron Muon (E-665) Experiment:

The spectrometer[1], shown in Fig. 2, is based on two large superconducting dipoles, the CERN Vertex Magnet (CVM) and the Chicago Cyclotron Magnet (CCM). Tracking was accomplished with multi-wire proportional counters, drift chambers and a vertex streamer chamber. For particle identification there were two threshold Cerenkov counters as well as a large ring imaging Cerenkov (RICH) counter.

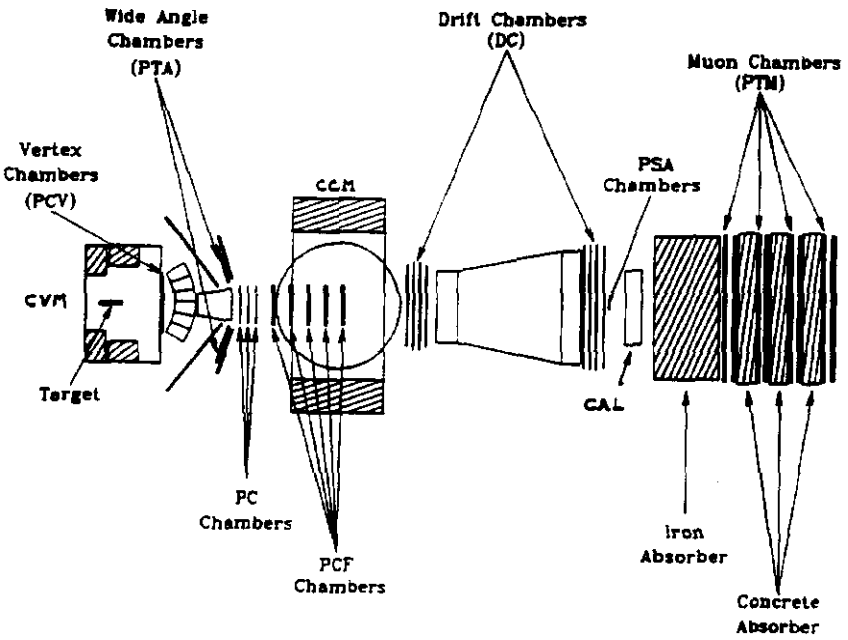

Fig 2. Plan view of the E-665 Detector

The experiment used an incoming beam of muons, $\approx$ 1 MHz, with $< E_\mu >$ = 490 GeV scattering off H_2, D_2 and Xenon targets. The combination of forward plus vertex spectrometers, yielded $\approx 4\pi$ geometrical acceptance. The trigger acceptance for both the Large Angle Trigger (LAT) and Small Angle Trigger (SAT) is shown in fig. 3 below. The most significant kinematic characteristic for the studies discussed in this paper is the range in hadronic CM energy (W) which goes as high as 35 GeV, comparable with PEP/PETRA energies. Radiative corrections, based on Mo & Tsai[2], were performed with a maximum correction of 20% when a $y < 0.85$ cut was made. Monte Carlo simulation was performed using the Lund Monte Carlo with Morfin-Tung[3] parton distributions.

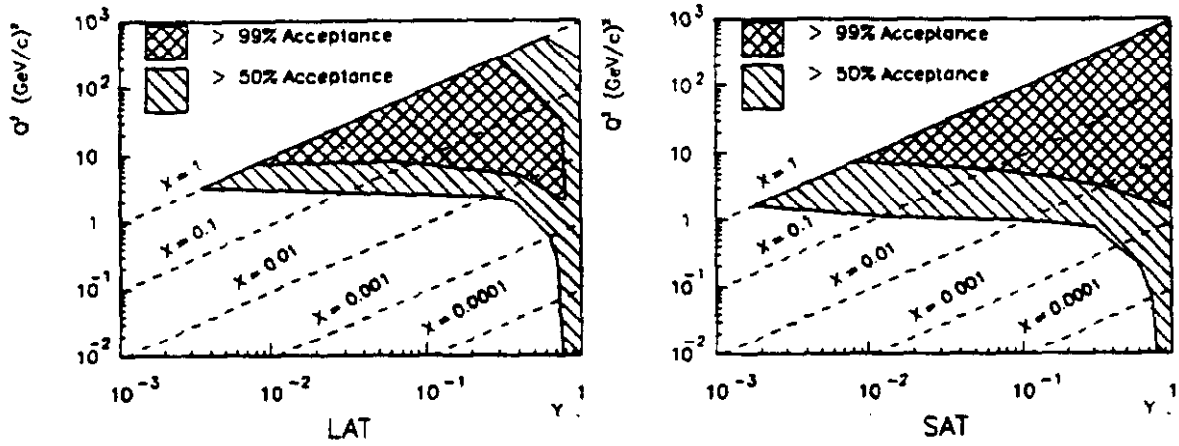

Fig 3. The kinematic trigger acceptance of the SAT and LAT

3 Space-time Evolution of the Hadronization Process

3.1 Theory

By studying the space-time development of a high energy muo-produced hadron shower, we are trying to answer two fundamental questions about the nature of the quark. First, what is the **quark**-nucleon cross section? Second, when does the struck quark start fragmenting into hadrons? It will become obvious that a study of nuclear effects is crucial for answering the above two questions. Experimentally we are trying to determine what happens between the time a muon is detected as scattering

within the experimental target and a shower of hadrons emerges. The process can be divided into three stages:

1. The muon transfers a fraction of its energy to a parton.
2. The parton travels through the nuclear medium and hadronizes.
3. The hadrons continue the passage through the target material and emerge.

Stage 1 covers such topics as the hadronic nature[4] of the photon which mediates the deep inelastic interactions and the measurement of the nucleon structure function[5]. These results tell us the probability with which the photon will interact with a quark of a given flavor and what fraction of the total nucleon's momentum will be carried by the quark. Stage 3 has been studied for many years and is covered well by references[6] dealing with the passage of a particle through matter. Naturally stage 3 phenomena also includes hard final state scatters which would take us back to stage 2 ... etc.

The significance of a space-time analysis of high energy processes as well as the basic ideas were summarized by Bjorken[7] in several reports from the mid 70's. He pointed out the importance of long time intervals and large distances which had been emphasized earlier by Landau and colleagues[8]. At the time, the emission of hard hadrons was postulated to be a tail effect of a bremsstrahlung-type process of soft hadron emission. In this case, the distance required for the hadron to form in the lab is simply the time/distance for the quark to fragment to the hadron in the quark rest frame - a distance of $\approx 1/m_h$ - boosted by its Lorentz factor (E_h / m_h) into the lab. This hypothesis was consistent with the observed[9] absence of intranuclear cascading of high energy hadrons since, if $E_h/m_h^2 >$ nuclear size, the hadron is formed outside of the nuclear matter.

A series of increasingly complex models[10] followed these early concepts. They attempt to describe the behavior of leading hadrons with large z (or x_F). In 1980 Nikolaev[11] applied the formation length concept to lepton-nucleus interactions. Bialas[12] introduced 2 cross sections in addition to the formation length. The parameter σ_q the quark-nucleus cross section and σ_h the hadron-nucleus cross section. The first attempt to derive an analytic expression for the time of formation by Bialas and Gyulassy[13] used the Lund fragmentation model. There are, unfortunately, as of yet no models based on QCD since the current methods of perturbative expansion are not valid for hadronization. We are thus left with a picture which can be summarized by the following figure:

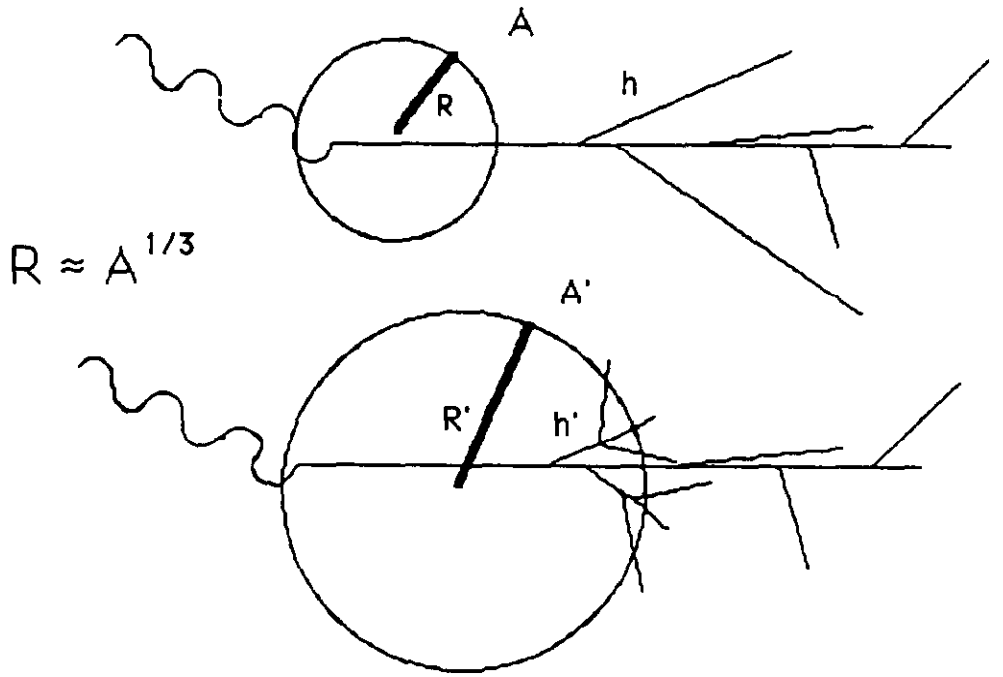

Fig.4 The struck quark travels out of nucleus A before hadronizing but hadronizes within nucleus A' with resultant interaction of produced hadron h'

3.2 Experiment

(From the Doctoral thesis of **Alexandro F. Salvarani**, U. of CA, San Diego)

The main thrust of this phase of the experiment was to study the ratios of multiplicity distributions of hadrons produced in the scattering of muons off of different nuclei. Examined was the ratio of differential multiplicity distributions

$$R_{A_1/A_2}(z) = \left(\frac{1}{N_\mu} \frac{dn}{dz} \right)_{A_1} / \left(\frac{1}{N_\mu} \frac{dn}{dz} \right)_{A_2}$$

and, to emphasize any nuclear effects on the leading hadrons, the ratio of integrated z distributions

$$\overline{R}_{A_1/A_2}(z_{min}) = \int_{z_{min}}^{1.0} dz \left(\frac{1}{N_\mu} \frac{dn}{dz} \right)_{A_1} / \int_{z_{min}}^{1.0} dz \left(\frac{1}{N_\mu} \frac{dn}{dz} \right)_{A_2}$$

The charged particles with $x_F > 0$ from a sample of 10,000 Xe and 10,000 D_2 events with:

$$\nu > 20\ \text{GeV}$$
$$y < 0.8$$
$$Q^2 > 2\ \text{GeV}^2/c^2$$
$$x_{Bj} > 0.003$$

were studied.

The results of the analysis can be summarized with the following figures. Fig. 5 shows the ν and p_t^2 dependence of nuclear effects in the integrated z distributions. For a $z > 0.4$ cut, there is a definite depletion in R and the hint of an enhancement in the ratio of average p_t^2 for low values of ν. The lack of any A dependence in $\overline{R}_A$ at large ν is a strong indication that, for large energy transfer to the quark, the hadrons created via fragmentation are not seeing nuclear matter. Fig. 6 shows the data as a function of Q^2 and x_{Bj}. No significant dependence is seen indicating that the phenomena is, most likely, not a scaling violation effect or dependent on the quark flavor.

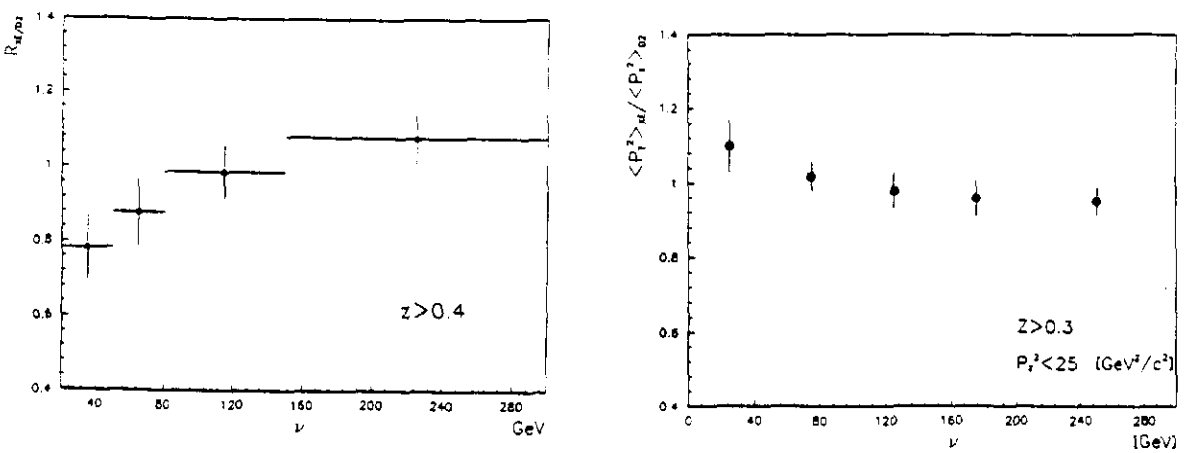

Fig.5 $\overline{R}_A$ and the ratio of average p_t^2 as a function of ν for a $z > 0.4$ cut

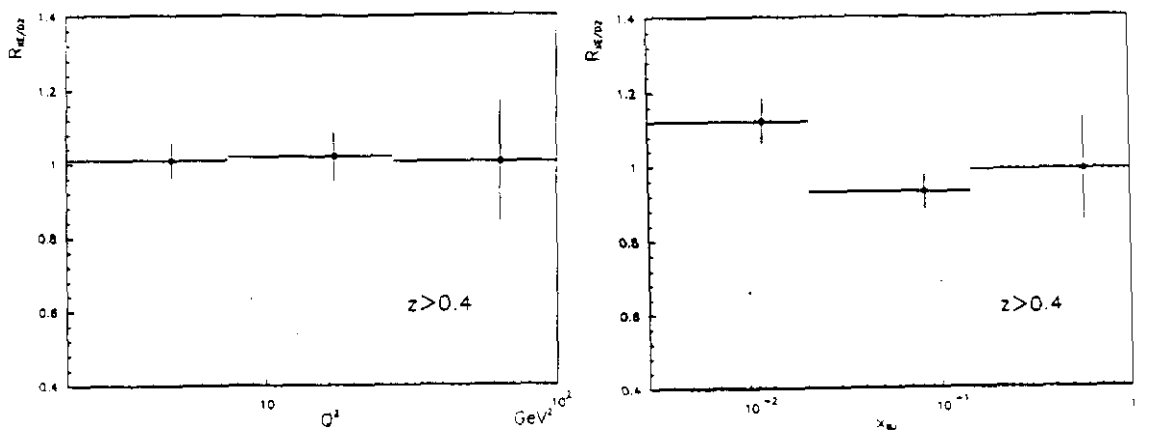

Fig.6 $\overline{R}_A$ as a function of Q^2 and x_{Bj} for a $z > 0.4$ cut

The conclusions of this study can be summarized as follows:

1) There is a depletion of $(18 \pm 8)\%$ in leading hadrons when comparing Xenon to Deuterium at low n.

2) For $\nu > 50$ GeV, the Xenon and Deuterium z and p_t^2 distribution are essentially equal, consistent with the hypothesis that hadronization takes place outside the nucleus.

3) The ratio is independent of Q^2 and x_{Bj} indicating that the attenuation is most likely neither a scale violating effect nor a function of quark flavor.

4) There is a hint that $< p_t^2 >$ is larger in Xenon than in Deuterium at low ν, again consistent with the concept that the depletion of leading hadrons is caused by rescattering within the nucleus.

THESE PRELIMINARY RESULTS ARE CONSISTENT WITH THE HYPOTHESIS THAT THERE IS A FINITE HADRONIZATION LENGTH AND IT IS PROPORTIONAL TO ν.

4. Leading hadron distributions in Shadowing Region.

4.1 Theory

When one observes the cross section ratio of either hydrogen or deuterium to a much heavier nucleus there are various visible effects, seen as excursions from unity in the ratio, as one proceeds from high to low x_{Bj}. There is a rise in the region ($.6 < x_{Bj} < 1.0$), a depletion in the region ($.2 < x_{Bj} < .6$), a "bump" in the region ($.1 < x_{Bj} < .2$) and, finally, a depletion for the very low x region ($x_{Bj} < .01$). These excursions are due to Fermi motion, the so-called EMC effect, anti-shadowing and shadowing respectively.

It is this last phenomena, shadowing, that is of interest to us here. In hadron-nucleus interactions shadowing has long been observed[14] and is assumed to be due to the nature of the interaction, which is strong, so that scattering will occur near the surface of the target nucleus. The upstream part of the nucleus "shadows" the downstream part so that the cross section varies as a function of the surface area and not the volume of the nucleus i.e. $A^{2/3}$ rather than $A^{1.0}$. This would imply that the per-nucleon cross section on nuclear targets would be smaller than that of the free nucleon.

In muon scattering the 4-momentum is transferred from the muon to the quark (nucleus) via a virtual photon in an, ostensibly, non-strong interaction so that one would not expect shadowing to occur as in hadron nucleus interactions. However, shadowing **has** been observed in real photon absorption cross sections as well. This has historically been described as Vector Meson Dominance[15], the photon transforms into a virtual meson with the same quantum numbers as the photon. In this model one would expect a rather strong dependence of the phenomena on Q^2 . There have also been attempts to describe the shadowing phenomena in the framework of Quantum Chromodynamics (QCD). This has been accomplished with the use of "recombination" functions[16] which demonstrate how partons from neighboring nuclei recombine. The effect becomes more noticeable as x_{Bj} becomes smaller since the smaller x_{Bj} the smaller the momentum of the quark and the more imprecise its spatial localization. When the localization becomes large with respect to nuclear size the partons can overlap with partons in neighboring nuclei and recombine. This results in a net depletion of the small x_{Bj} partons in nucleons of a nucleus compared to free nucleons. The model predicts a very weak Q^2 dependence which would discriminate between VMD and QCD models.

4.2 Experiment

(From the Doctoral thesis of **John J. Ryan**, Massachusetts Institute of Technology)

In addition to manifesting itself in the ratio of cross sections, shadowing could conceivably alter the distribution of observed hadrons. Experiments in hadron-nucleus scattering that have observed shadowing in the ratio of cross sections have also observed[17] a correlated attenuation of the final state hadrons. The Tevatron Muon Collaboration has attempted to detect and measure the shadowing phenomena both in the ratio of cross sections and in the final state hadrons of muon nucleus interactions.

Due to the comparatively high energy of the incoming muons the Tevatron Muon Experiment is able to reach very low values of x_{Bj} . Fig. 7 shows the ratio of Xenon to Deuterium cross sections in the range ($5 \times 10^{-4} < x_{Bj} < 0.15$). The shadowing effect at low x_{Bj} is clear and there is an indication for anti-shadowing in the vicinity of $x_{Bi} = .06$.

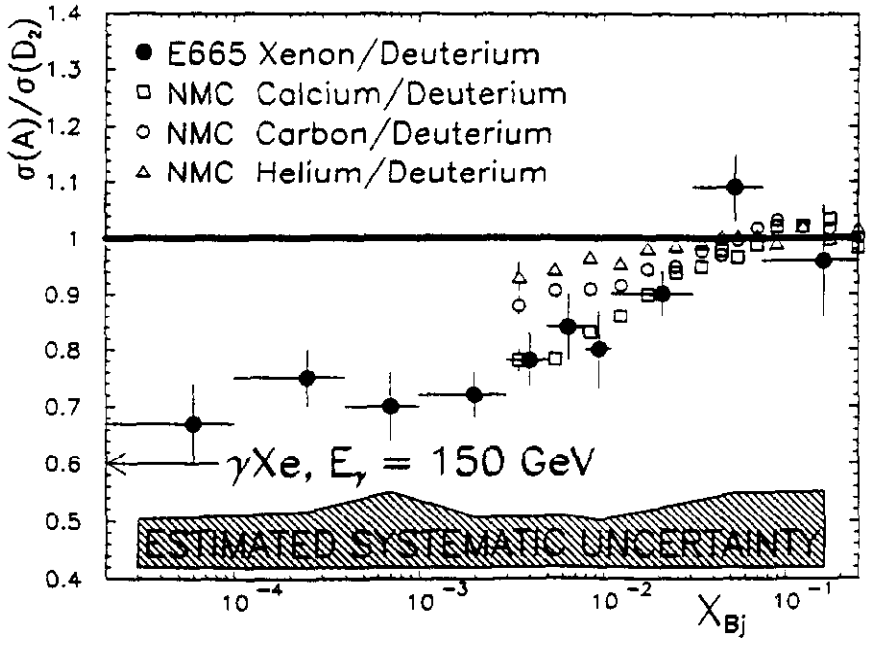

Fig.7 The ratio of Xenon to Deuterium cross sections as a function of x_{Bj}

To investigate the differences in the hadron shower between interactions in the shadowing and non-shadowing regimes, two kinematic regions were chosen. The first is defined by $x_{Bj} < 0.005$, $Q^2 < 1$ GeV^2 / c^2 while the non-shadowing region is $x_{Bj} > 0.03$, $Q^2 > 2$ GeV^2 / c^2. As can be

seen from Fig. 7 these are reasonable regions to compare. The sample analyzed was approximately 20,000 deuterium and 17,000 xenon tracks. Comparisons were made between the ratio of z distributions of hadrons from the xenon sample to hadrons from the deuterium sample in the two kinematic regions. If there is an effect in the hadronic jet correlated to the clear evidence for shadowing seen in the cross sections, there should be a difference in the ratios in the 2 kinematic regions.

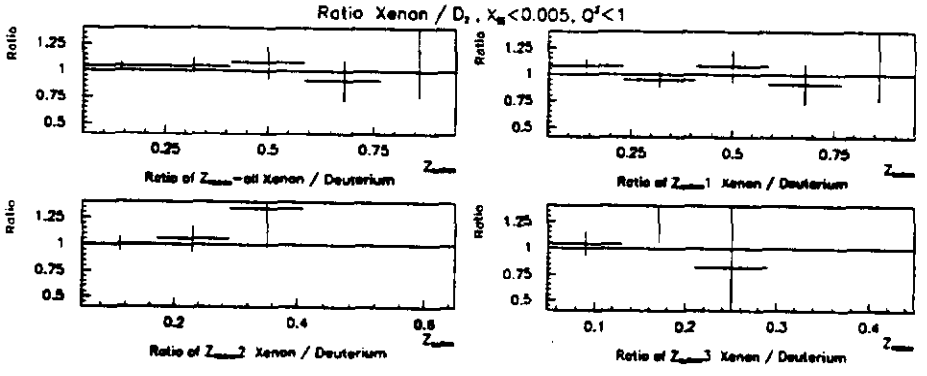

Fig. 8 Z Distributions of the ratio of Xe/D2 in the shadowing region

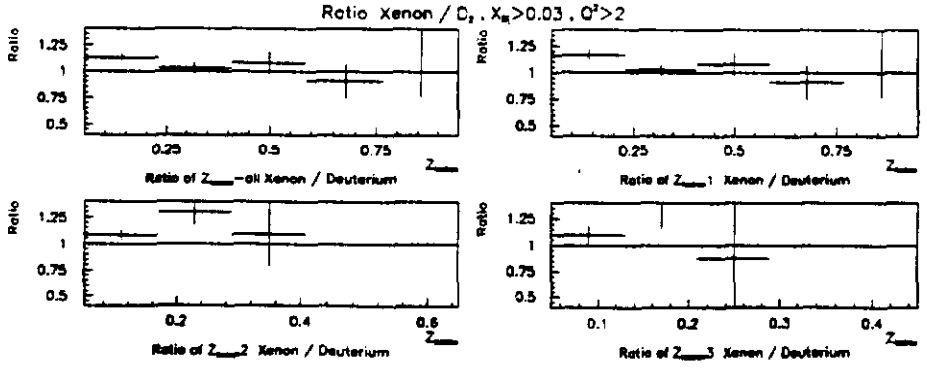

Fig. 9 Z Distributions of the ratio of Xe/D2 in the non-shadowing region

The conclusion to be drawn from this analysis of the Z distributions of the final state hadrons is that they show no evidence for a target dependence even in the shadowing region where a strong shadowing effects are evidenced in the ratio of total cross sections. Looking at the implications of sections 3 and 4 we can draw the following overall conclusions:

1) Nuclear shadowing is a well established phenomena and is consistent with a parton rather than a VMD model interpretation.

2) Although nuclear matter is very absorbing for a hadronic system in general, it is very transparent to fast quarks.

3) Quarks which have absorbed energies of less than ≈ 50 GeV either produce hadrons within a nuclear radius or are attenuated.

4) There is no measurable difference in the distributions of fast hadrons produced in the shadowing region compared to those produced in the non-shadowing region. Since this occurs for large quark energies, it may be an indication that the quark-nucleon cross section is very small.

5. Rates and Characteristics of 3-jet Events

The Tevatron Muon Collaboration has recently completed the first measurement[18] of multi-jet rates produced by deep-inelastic muon scattering. The simple Quark Parton Model predicts a backward jet and only one forward jet. Leading order QCD corrections[19] introduce additional sources of multi-forward jet phenomena; gluon bremsstrahlung and photon-gluon fusion. The rates of 3-jet events are a function of $\alpha_s(Q^2)$, the running strong coupling constant, and the parton distribution functions.

After the standard cuts to enhance the deep-inelastic sample:

$$\nu > 40\ \text{GeV}$$

$$y < 0.95$$

$$Q^2 > 4\ \text{GeV}^2/c^2$$

$$x_{Bj} > 0.003$$

there were a total of 12,600 events with an average multiplicity of 5.4 particles. Only forward going particles in the CM system with lab energy greater than 2 GeV were used in the subsequent analysis.

The method employed to define jets was the JADE algorithm[20] which uses the scaled invariant mass of pairs of particles in the virtual photon-proton CM system;

$$y_{ij} = \frac{M_{ij}^2}{s^2}, \qquad M_{ij}^2 = 2 E_i E_j (1 - \cos \phi_{ij})$$

with all charged particles assumed to be pions and neutral particles to be photons. If the y_{ij} is less than a chosen y_{cut}, the particles i and j are combined into a single psuedo-particle with 4-moment equal to the sum of the 4-momenta of particles i and j. This procedure is repeated until y_{ij} is greater than y_{cut}. The resulting psuedo-particles are called "jets".

The LUND[21] (LEPTO 5.2 and JETSET 6.3) Monte Carlo with Morfin-Tung parton distributions was used to generate physics events which were then passed through a GEANT[22] based simulation of the detector to correct the data for resolution, reconstruction efficiency and geometrical acceptance. To check the sensitivity of the 3-jet rate to the physics generator employed, both a leading order QCD matrix element method and a QCD parton shower method were used to generate events.

Fig. 10 shows the rate of 1, 2, and 3 forward jet events as a function of y_{cut} and for different ranges of the hadronic invariant mass W. Note that as y_{cut} increases, more and more (pseudo-) particles must be combined to survive the cut and, eventually, only "1 forward-jet" events are left. For a given y_{cut} the change in the observed rate of 2 forward-jet events as a function of W can be compared with Monte Carlo predictions. Leading order PQCD[23] predicts that the 2 forward-jet rate falls as W increases when the JADE algorithm is used to define jets. This is true whether one uses the matrix element or the parton shower methods, as can be seen in Fig. 11 which displays this rate as a function of W for a value of $y_{cut} = 0.04$. The experimental points, corrected with the matrix element based Monte Carlo, are in excellent agreement with both the matrix element and the parton shower predictions. Fig. 11 also displays the simple quark parton model predictions (no QCD), using the LUND Monte Carlo, which are in strong disagreement with the measured points.

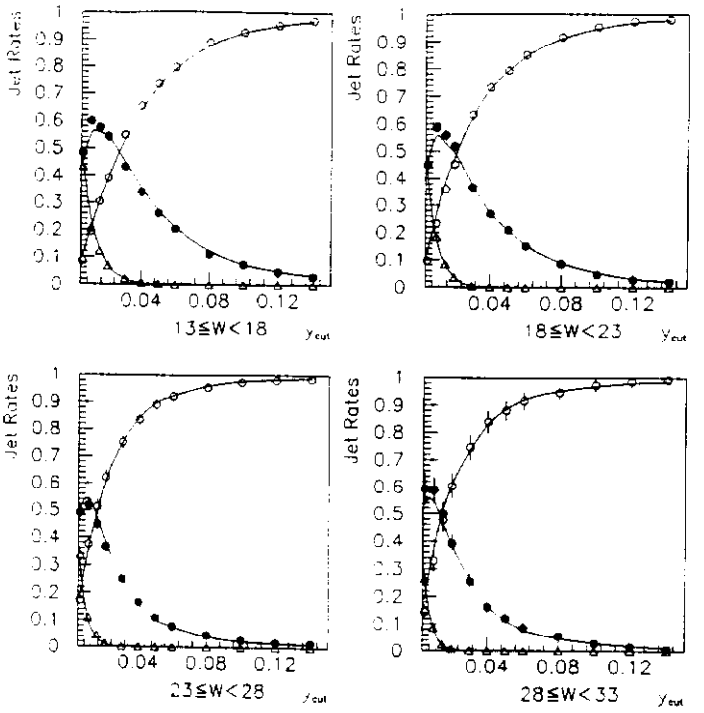

Fig. 10 Corrected Rates of 1-jet (O), 2-jet (•) and 3-jet (Δ) production as a function of y_{cut} for various W bins.

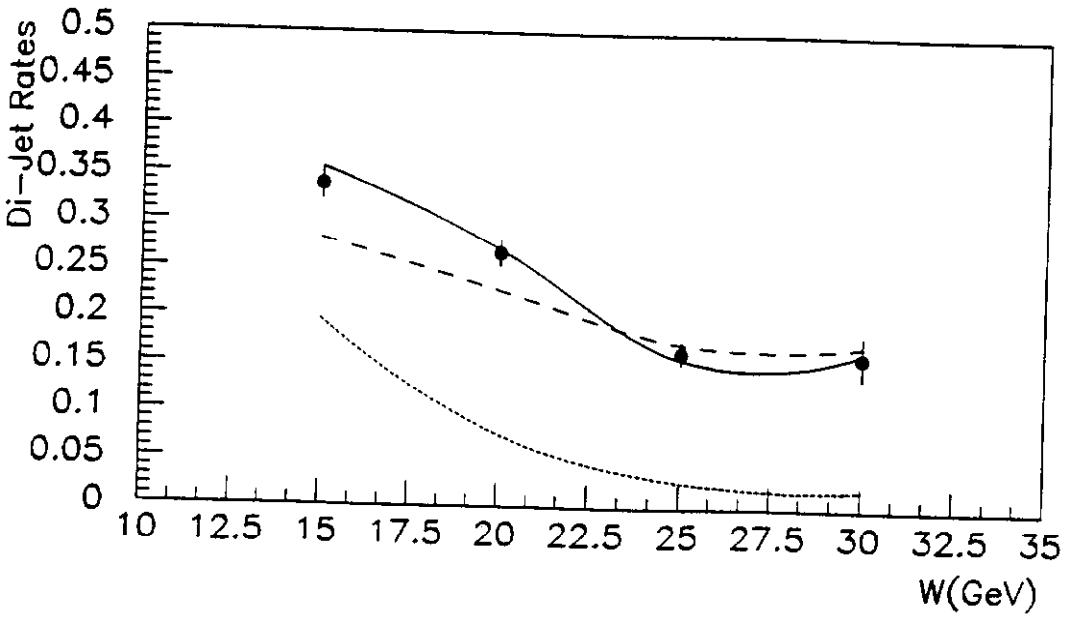

Fig. 11 Corrected 2-jet rates vs W compared to LUND ME (solid), LUND PS (dashed) and without QCD (dotted) predictions

6. Acknowledgements

I would like to sincerely thank the organizers of this conference not only for the well structured sessions and fascinating social functions but also for giving me my first opportunity to meet the very warm and friendly people of China at home. In particular I would like to mention **Prof. Weiqin Chao, Mr. Chen, Ms. Peng Song and Ms. Shuhui Song** for their kind hospitality.

7. References

1. M. R. Adams et al., *Nucl. Inst. Meth.* **A291** (1990) 533.
2. L.W. Mo and Y.S. Tsai, *Rev, Mod, Phys.* **41** (1969) 205.
3. J.G. Morfín and W.K. Tung, *Z. Phys.* **C52** (1991) 13.
4. T. Sloan, *Recent Results in Deep Inelastic Scattering,* CERN **EP/86-111**
5. For a recent summary of the topic see R.G. Roberts and M.R. Whalley, *A Compilation of Structure Functions in Deep-inelastic Scattering, J. Phys.* **G17** (1991) D1.
6. E. Segre, *Nuclei and Particles*, W.A. Benjamin, New York, 1984.
7. J.D. Bjorken, SLAC-**PUB-1756**, May 1976.
8. L.D. Landau, *IZV. Akad. Nauk. SSSR* **17** (1953) 31.
9. W. Busza, *Acta Phys. Pol.* **B8** (1977) 333.
10. A. Dar and F. Takagi, *Phys. Rev. Lett.* **44** (1980) 768; G. Nilsson et al., *Phys. Lett.* **83B** (1979) 379.
11. N.N. Nikolaev, *Z.Phys.* **C5** (1980) 291.
12. A. Bialas and E. Bialas, *Phys Rev.* **D21** (1980) 675; A. Bialas, *Acta Phys. Pol.* **B11** (1980) 475.
13. A. Bialas and M. Gyulassy, *Nucl. Phys.* **B291** (1987) 793.
14. W. Kittel, *Act, Phys. Pol.* **B12** (1981) 1093.
15. D. Perkins, *Introduction to High Energy Physics*. Addison-Wesley, 1982.
16. F.E. Close et al., *Phys. Rev.* **D40** (1989) 2820.
17. W. Busza, *Acta Phys. Pol.* **B8** (1977) 333.
18. C. W. Salgado, *The JADE Algorithm Jet Rates*, E-665 Internal Report; The E-665 Collaboration, *Jet Production Rates in Deep Inelastic Muon-Proton Scattering*, Submitted to Phys. Rev. Lett.
19. J.G. Koerner et al., *Int. J. Mod. Phys.* **A4** (1989) 1781.
20. W. Bartel et al., *Z. Phys.* **C33** (1986) 23.
21. T. Sjostrand, *Comp. Phys. Comm.* **27** (1982) 243.
22. R. Brun et al., *GEANT Manuel*, CERN (1986).
23. T. Brodkorb et al., *Z. Phys.* **C44** (1989) 415.